International Journal of Power Electronics and Drive System (IJPEDS)
Vol.2, No.1, March 2012, pp. 107~116
ISSN: 2088-8694

Torque Analysis of Permanent Magnet Hybrid Stepper Motor using Finite Element Method for Different Design Topologies

E. V. C. Sekhara Rao*, Dr P. V. N. Prasad**
* Assistant Professor, Department OF Electrical & Electronics Engineering, CBIT, Kokapeta Post, Hyderabad-75, India
** Professor, Department of Electrical Engineering, UCE, Osmania University, Hyderabad -07, India

Article Info

Article history:

Received Nov 2nd, 2011
Revised Feb 27th, 2012
Accepted Mar 9th, 2012

Keyword:

Cogging torque
FEM
Instantanious Torque
PDE toolbox
Permeance model

ABSTRACT

This paper discusses about permanent magnet hybrid stepper motor magnetic circuit using finite element method for different geometric designs like uniform air-gap, non uniform air-gap, for different air-gap lengths, different tooth pitches and extra teeth on stator using PDE toolbox of Matlab at different current densities. Implementing these results in equivalent circuit model (permeance model), motor performance is analyzed for an existing motor for steady state conditions. These results suggest modifications for better performance of the PMH stepper motor like reduction of cogging torque and improvement in steady state torque with minimum THD

Corresponding Author:

E. V. C. Sekhara Rao
Assistant Professor, Department OF Electrical & Electronics Engineering,
Chaitanya Bharathi Institute of Technology,
Kokapeta Post, Hyderabad-500075, India.
Email: chandrasekharev@yahoo.co.in, chandrasekhar.ev@gmail.com

1. INTRODUCTION

Stepper motors are used in a variety of applications, including high and low propulsion technology, solar array tracking system in satellites, computer peripherals, machine tools, robotics, etc. Stepper Motors are divided into two major groups, one without permanent magnet and the other with permanent magnet. The term hybrid is derived from the fact that the motor is operated under the combined principles of permanent magnet and variable reluctance motors. The motor having the permanent magnet rotor and multiple teeth both on the stator and rotor poles, with excitation in stator poles is called the hybrid stepper motor.

Hybrid stepper motors (pmh) are highly preferred in space applications as they can provide accurate positioning in open loop system [1]. The positional accuracy of the stepper motors will be high only when its step angle is very small. Hence for space applications hybrid stepper motor is the best choice as it can offer small step angles in the range of 0.5^0 to 1.8^0.The other classes of stepper motors such as variable reluctance stepper motor and permanent magnet stepper motor will be suitable only for applications which require large step angles.

The design of a hybrid stepper unlike that of conventional ac motors such as induction motor and synchronous motor using equivalent magnetic circuit analysis is not easy because of the complex air-gap geometry, which results in complex air-gap permeance variation [2]. Because of this, analysis using electromagnetic computation is a complex task and these results in the dependency of FEM technique for design and analysis..

Since hybrid stepper motor has a large number of teeth on the stator and rotor surface and a very small air gap, the magnetic saturation in the teeth becomes severe while increasing the flux density in the air-gap.

In addition both radial and axial flux is produced because of axially magnetized permanent magnet and geometric characteristics

This makes the analysis of hybrid stepper motor more difficult using 2D FE modeling. Three dimensional FE analyses is one of the solutions for nonlinear analysis of axially unsymmetrical hybrid stepper motor under this situation. But in order to reduce the computational time involved in the analysis a 2D equivalent of the 3D model of the motor was developed and used.

2. FEM OF HYBRID STEPPER MOTOR

Tooth layer unit (TLU) [3] is a rectangle area that has a tooth pitch width and two parallel lines behind the teeth of stator and rotor. The area is shown in Fig.1.The factors of the nonlinear material and the non-uniform distribution of magnetic field in the teeth of stator and rotor are taken full consideration in this computation model. There are two basic assumed conditions in the computation model of TLU.1.The lines AB and CD of the TLU in Fig.1 are considered as iso-potential lines.2. The magnetic edge effect of stator pole is ignored, which is assumed that the distribution of the magnetic field for every tooth pitch width is the same.

In Fig.1, u_s and u_r are the scalar quantities of the iso-potential lines AB and CD. The magnetic potential difference F is given in (1).

$$F = u_s - u_r \qquad (1)$$

If Φ (α) is assumed as the flux in a tooth pitch width per axial unit length of iron core and α is the relative position angle between stator and rotor, then the specific magnetic conductance G of TLU is given in (2).

$$G = \frac{\Phi(a)}{F} \qquad (2)$$

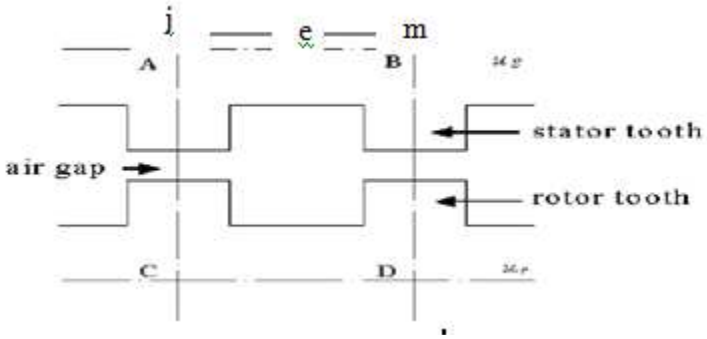

Fig.1. Tooth layer unit

Apparently, G is related to the saturation extent of iron core and is changed with F and the relative position angle α and it can be obtained by the numerical computation on the magnetic field of TLU shown in Fig.1 [3]. The lines AC and BD are the periodic boundary lines because the distribution of the magnetic field is considered as the same for every tooth pitch width. The magnetic field in TLU is irrational field and the magnetic equations for the field are given in the rectangular coordinates in (3).

$$\left.\begin{array}{c} \frac{\partial}{\partial x}\left(\mu\frac{\partial \boldsymbol{\varphi}}{\partial x}\right)+\frac{\partial}{\partial y}\left(\mu\frac{\partial \boldsymbol{\varphi}}{\partial y}\right) \\ \varphi_{CD}=0 \\ \varphi_{AB}=0 \\ \varphi\,(x,y)_{AC}=\varphi\,(x+\lambda,y)_{BD} \end{array}\right] \qquad (3)$$

where φ is the scalar quantity, μ is the magnetic permeability and λ is the tooth pitch. For a certain position angle α and a magnetic potential difference F, the distribution of the magnetic field of TLU can be calculated by the 2D finite element analysis. The flux per axial length of TLU is given in (4).

$$\varphi(\alpha,F)=\sum B_e\ \ (\overleftarrow{jm})_e \qquad (4)$$

Here the nodes j and m are on the border AB as shown in Fig1. $(\overline{jm})$ is the length of unit e from node j to m and B_e is the flux density. The specific magnetic conductance G will be used in the calculation of the whole nonlinear network equations of the motor.

3. RESULTS AND ANALYSIS

a. Design of Hybrid Stepper Motor

A practical 1.8^0 (mechanical) PMH stepper motor is chosen for design. It has 4 poles in the stator and 2 sections in the rotor with $AlNiCo_5$ magnet axially magnetized. The main structure parameters of the motor are shown in Table1

Table 1: Data of PMH Stepper Motor

Stator poles	Tooth per stator pole	Outside diameter of stator	Inside diameter of stator	Outside diameter of stator shell
04	8	10.108 cm	5.936 cm	10.652 cm
Tooth number of rotor	Number of turns per phase	Section length of rotor	Outside diameter of rotor	Inside diameter of rotor
50	46	10.26 cm	4.2 cm	1.74 cm
No of turns per stator pole	Rated voltage	Rated current	SWG of conductor	Torque
92	12 V	1 A	36	1.5 Nm

PDE toolbox of Matlab for FEM analysis is used to investigate mmf due to permanent magnet for different topologies which is difficult to investigate by mathematical model [4]. Different topologies considered are 1) Uniform air-gap (0.137 mm) with extra teeth on stator 2) Uniform air-gap (0.137 mm) without extra teeth on stator 3) Non-uniform air-gap (0.137 mm) with extra teeth on stator 4) Non-uniform air-gap (0.137 mm) without extra teeth on stator 5) Uniform air-gap (0.93 mm) with extra teeth on stator 6) Uniform air-gap (0.93 mm) without extra teeth on stator 7) Non-uniform air-gap (0.93 mm) with extra teeth on stator 8) Non-uniform air-gap (0.93 mm) without extra teeth on stator. The details of all the eight topologies are shown in Table 3.

All topologies are investigated with Iron (99.8%) and Iron (99.95%), for rare earth permanent magnets NdFeB, Sm_2Co_{17} at current capacities of 0.5 A and 1 A. The related magnetic potential diagrams are shown from Fig. 2 to Fig. 5 for one / two iron core materials (99.8% and 99.95%) with NdFeB as permanent magnet. Fig. 2 shows for Uniform air-gap (0.137 mm) with extra teeth on stator without excitation. Fig. 3 shows for uniform air-gap (0.137 mm) with extra teeth on stator with excitation of 0.5 A. Fig. 4 shows for uniform air-gap (0.137 mm) without extra teeth on stator without excitation and Fig. 5 shows for uniform air-gap (0.137 mm) without extra teeth on stator with excitation of 0.5 A. Similarly for all remaining topologies, for different core materials and different permanent magnets at different current densities, magnetic potential is investigated with and without excitation. This magnetic potential is multiplied with axial length (10.26 cm) and air-gap lengths (0.137 mm, 0.93 mm) to get total mmf.

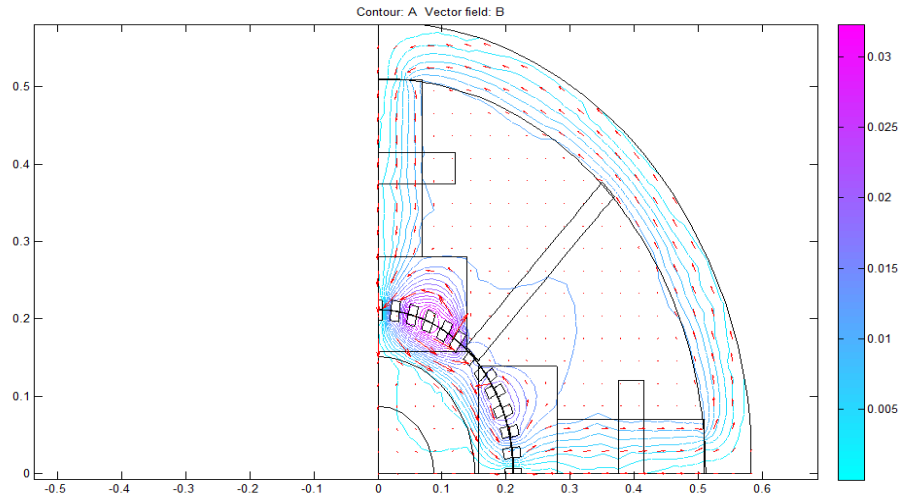

Fig. 1. Magnetic potential as contour and flux density as arrows of PMH motor for topology 1 without excitation for two core materials, iron (99.8%), Iron (99.9) for NdFeB permanent

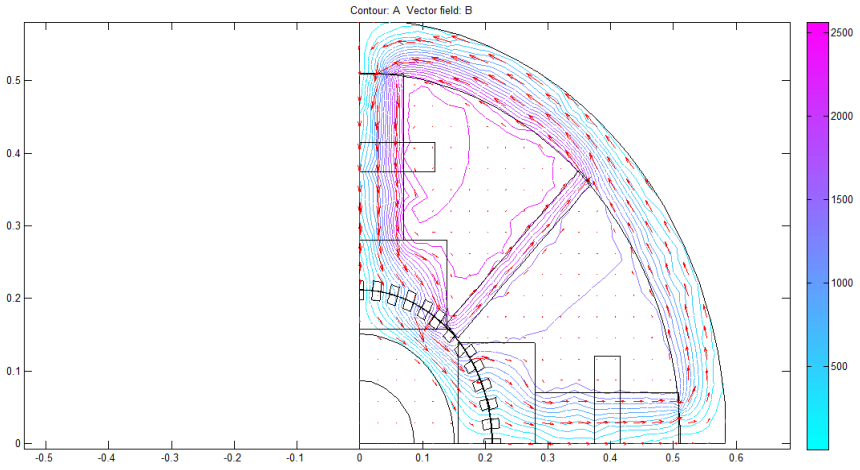

Fig.3. Magnetic potential as contour and flux density as arrows of PMH motor for topology 1 with excitation of 0.5A for core material, iron (99.8%) for NdFeB permanent magnet

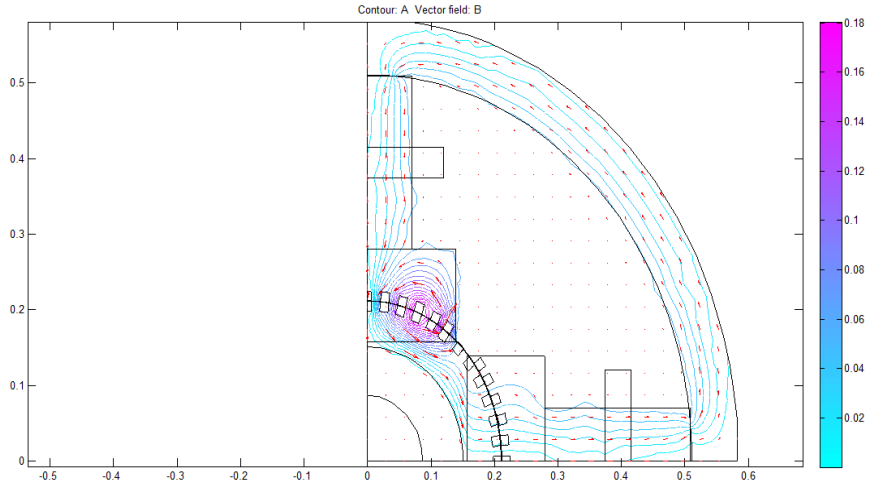

Fig.4. Magnetic potential as contour and flux density as arrows of PMH motor for topology 2 without excitation for two core materials, iron (99.8%), Iron (99.9%) for NdFeB permanent magnet

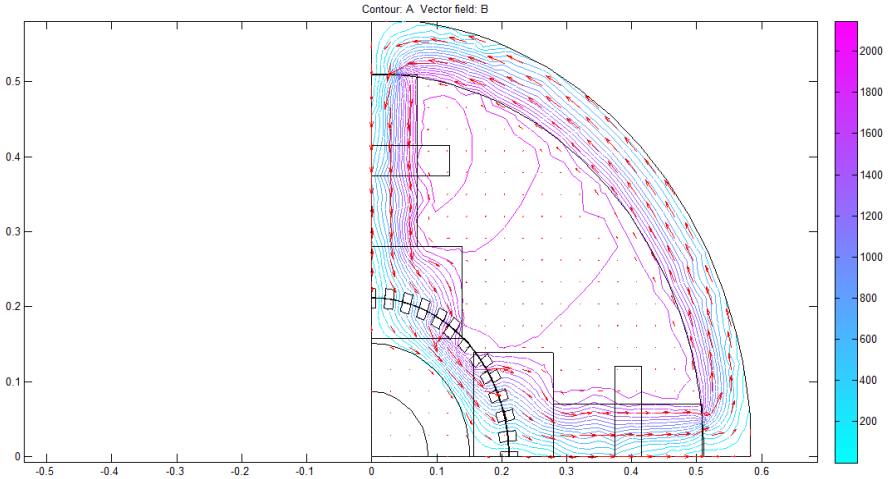

Fig. 5. Magnetic potential as contour and flux density as arrows of PMH motor for topology 1 with excitation of 0.5A for core material, iron (99.8%) for NdFeB permanent magnet

3.2. Permeance Model of Hybrid Stepper Motor

The gap permeances (P_1-P_5) [5] are calculated using (5) for the tooth layer unit shown in Fig.6 [6]

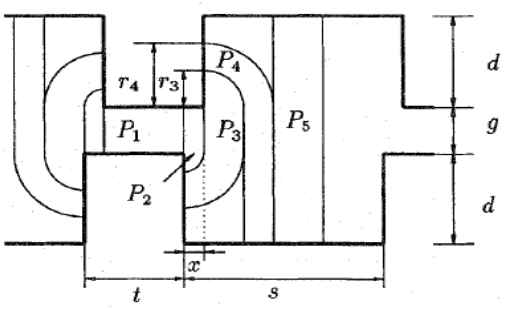

Fig.6: Linearized tooth layer unit arrangement and flux tubes

$$\left.\begin{aligned} P_1 &= \mu_0 \frac{t-x}{g} \\ P_2 &= \mu_0 \frac{2}{\Pi} \ln\left(1+\frac{\Pi x}{2g}\right) \\ P_3 &= \mu_0 \frac{1}{\Pi} \ln\left(\frac{g+2d-\frac{1}{2}\Pi x}{g+\frac{1}{2}\Pi x}\right) \\ P_4 &= \mu_0 \frac{2}{\Pi} \ln\left(\frac{g+2d}{g+2d+\frac{1}{2}\Pi x}\right) \\ P_5 &= \mu_0 \frac{s-x-\frac{4d}{\Pi}}{g+2d} \end{aligned}\right] \quad (5)$$

Here, x =equivalent length of step angle mm, tooth width, t = 1.32 mm, tooth pitch, s = 1.42 mm, tooth depth, d = 1.32 mm, air-gap length, g = 0.137 mm and 0.93 mm are considered for the analysis. Suppose that the number of teeth per stator pole is Z_s, the total permeance per pole, P_t is given in (6), considering P_1 to P_5 are in parallel

$$P_t = Z_s\,[P_l + 2(P_2 + P_3 + P_4) + P_5]\ \text{Wb/A} \quad (6)$$

The Permeance per pole per phase is given by (7)

$$P_\propto = P_t + \sum_{n=1}^{\infty} P_n \cos(n\theta) \quad (7)$$

Since the displacement is from θ = 0 to 2π radians corresponds to one-pitch of a tooth, the electric angle θ is related to the mechanical step angle θ_m, as in (8), where Z_r is the number of teeth of the rotor

$$\theta_e^0 = Z_r \theta_m^0 \quad (8)$$

The gap permeance Fourier coefficients (?) for all topologies are evaluated using (5), (6), (7) and (8) and tabulated in Table 2

Steady state torque and cogging torques are obtained using (9) and (10) respectively [5].

$$T_0 = -\frac{Z_r}{2}(NI)(B_0\,A_m)\frac{\rho_0}{\rho_1}\sin\theta_e \quad \text{Nm} \quad (9)$$

where Z_r is rotor teeth, N is turns per coil per phase, I is per phase current in A, B_0 is flux density of permanent magnet in Wb/m^2, A_m is area of permanent magnet in m^2, ρ_0 and ρ_1 are Fourier coefficients and θ_e is electrical angle in degrees.

$$T_{cog} = \frac{Z_r}{2}\left(\frac{P_m}{\rho_0}F_m\right)^2 \rho_4 \sin 4\theta_e \quad \text{Nm} \quad (10)$$

Where, P_m is permanent magnet permeance in Wb/A, F_m is mmf of permanent magnet in AT and ρ_4 is Fourier gap coefficient. Steady state torque and cogging torque are obtained using mmf of permanent magnet and mmf due to excitation from Table 3 for all topologies for two iron cores (99.8%, 99.95%) with

rare earth permanent magnets NdFeB and Sm_2Co_{17} at current capacities of 0.5 A and 1A. These results are tabulated in Table 3.

Table 2. Fourier coefficients of gap permeance for different topologies

Topology	Fourier coefficients of gap permeance					
	$\rho_0 \times 10^{-4}$	$\rho_1 \times 10^{-5}$	$\rho_2 \times 10^{-5}$	$\rho_3 \times 10^{-5}$	$\rho_4 \times 10^{-5}$	$\rho_5 \times 10^{-5}$
1	4.320	3.222	2.809	4.276	3.280	1.915
2	5.375	3.043	2.464	5.321	3.681	1.679
3	1.184	7.665	5.904	1.172	8.294	4.024
4	7.093	3.832	2.952	7.022	4.636	2.012
5	1.656	8.950	6.893	1.640	1.082	4.699
6	1.506	8.136	6.526	1.552	1.025	4.448
7	4.328	2.338	1.801	4.070	2.829	1.227
8	2.164	1.169	9.005	2.142	1.414	6.138

Fig.7 and Fig. 8 show the responses of permeances for topology 1 and 2 respectively. Fig. 9 and Fig. 10 are responses of steady state torque and cogging torque of iron core (99.8%) for topology 1 and topology 2 respectively at 0.5 A.

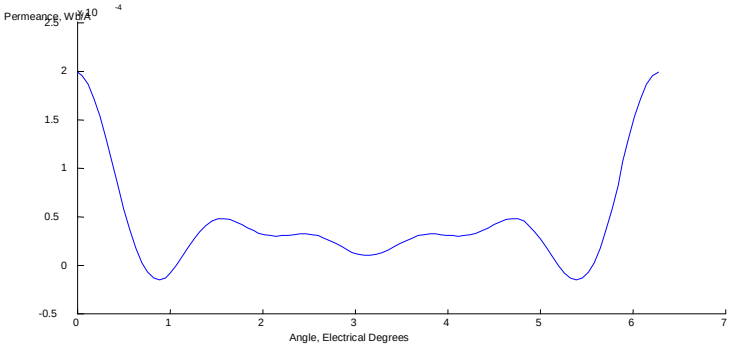

Fig.7. Permeances for topology 1

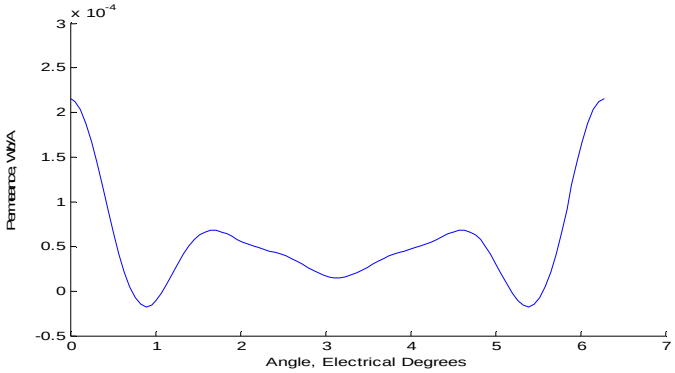

Fig.8. Permeances for topology 2

3.3. Instantaneous Torque of Hybrid Stepper Motor

Instantaneous torques of even harmonic and odd harmonic in Nm can be evaluated using (11), (12) [7] respectively

$$T_e = 2N^2 I^2\{(P_2 - 4P_4 + 3P_6)\sin 4\theta + (3P_6 - 8P_8 + 5P_{10})\sin 8\theta + (5P_{10} - 12P_{12})\sin 12\theta + \ldots.\} \quad (11)$$

$$T_o = 2N I F_m\{P_1 + (-3P_3 + 5P_5)\cos 4\theta + (-7P_7 + 9P_9)\cos 8\theta + (-11P_{11} + 13P_{13})\cos 12\theta\} \quad (12)$$

Total torque in Nm is investigated using (13)

$$T_t = T_e + T_o \quad (13)$$

Fig.11 and Fig.12 are the responses of T_e, T_o and T_t for topology 1 at 0.5A and for topology 2 at 0.5A respectively for iron core (99.8%).

Instantaneous torques are investigated using mmf of permanent magnet and mmf due to excitation from Table 3 for all topologies for iron (99.8%), iron(99.95%) for rare earth permanent magnets NdFeB, Sm_2Co_{17} for current capacities of 0.5A, 1A to calculate THD and tabulated in Table 3

MMF is found uniformly distributed in uniform small air-gap distribution. Maximum MMF is interacted between stator and rotor for uniform airgap topology. Steady state torque is varying with current density linearly for uniform air-gap topology for iron (99.8) type with Sm_2Co_{17} permanent magnet. When air-gap is increased steady state toque is lost and more harmonic in nature. Cogging torque is low for non-uniform low air-gap without extra teeth on stator topology with iron (99.8) stator and rotor core but very low steady state torque. Cogging torque is more than steady state torque for large non uniform air-gap topology.

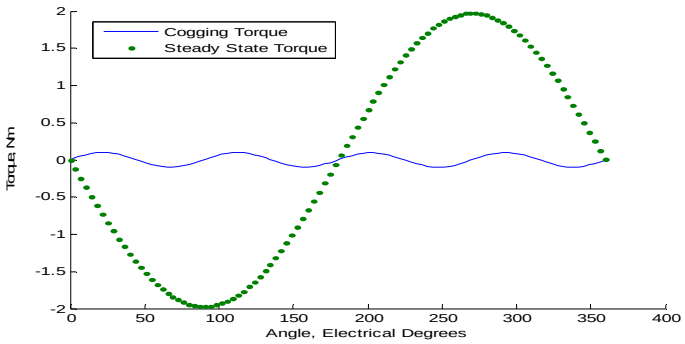

Fig.9. Steady state torque and cogging torque for topology 1 at 0.5A

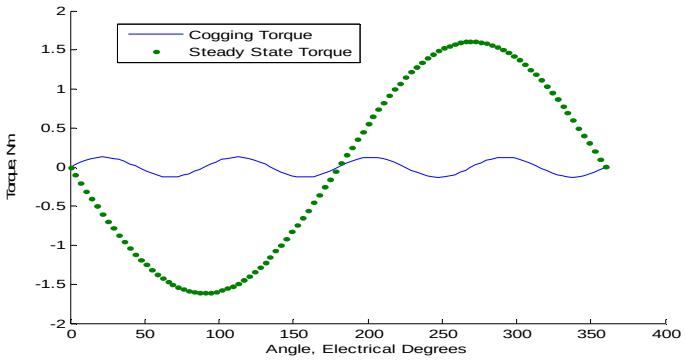

Fig.10. Steady state torque and cogging torque for topology 2 at 0.5A

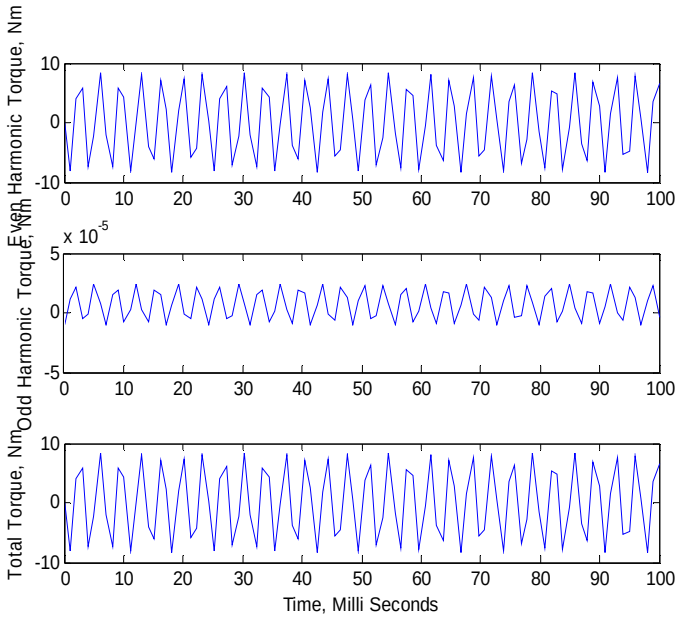

Fig 11.Instantaneous torques for topology 1 for 0.5A for iron (99.8%)

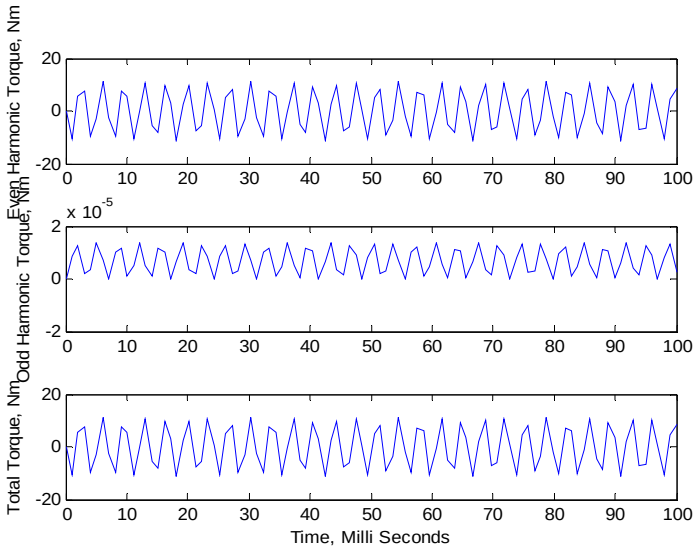

Fig.12. Instantaneous torques for topology 2 for 0.5A for iron (99.8%)

Table 3. MMF and Torque and THD of instantaneous torque for different topologies

Topology	Stator, rotor core Iron (%)	Permanent magnet	Current density (A/m^2)	MMF due to PM, $AT\times10^{-4}$	MMF due to excitation, AT	Instantanious torque THD **%**	T_0 (Nm)	T_{cog} (Nm)
		NdFeB	170648	4.578	23.6352	12.46	0.1596	0.0171
	Iron		341296	4.578	30.7940	15.57	0.1995	0.0171
	(99.8)	Sm_2Co_{17}	170648	4.578	23.6352	12.46	0.1596	0.0171
1			341296	4.578	30.7940	15.57	0.1995	0.0171
		NdFeB	170648	4.578	107.779	18.67	0.6982	0.0712
	Iron		341296	4.578	230.955	17.36	1.4960	0.0712
	(99.95)	Sm_2Co_{17}	170648	4.578	107.779	18.67	0.6982	0.0712
			341296	4.578	230.955	17.36	1.4960	0.0712
		NdFeB	170648	4.578	30.7940	10.78	0.2628	0.0982
	Iron		341296	4.578	38.4925	16.97	0.3285	0.0982
	(99.8)	Sm_2Co_{17}	170648	4.578	30.7940	10.78	0.2628	0.0982
2			341296	4.578	38.4925	16.97	0.3285	0.0982
		NdFeB	170648	6.159	92.3820	17.72	0.8051	0.1289

	Iron		341296	6.159	184.764	18.82	1.6100	0.1289
	(99.95)	Sm_2Co_{17}	170648	6.159	92.3820	18.01	0.8051	0.1289
			341296	6.159	184.764	17.16	1.6100	0.1289
		NdFeB	170648	1.232	15.3972	3.04	0.0320	0.0580
	Iron		341296	1.232	30.7940	6.08	0.0604	0.0580
	(99.8)	Sm_2Co_{17}	170648	1.231	15.3972	3.04	0.0320	0.0580
3			341296	1.231	30.7940	6.08	0.0604	0.0580
		NdFeB	170648	4.578	46.4910	3.67	0.2417	0.3631
	Iron		341296	4.578	92.3820	7.3	0.4803	0.3642
	(99.95)	Sm_2Co_{17}	170648	3.079	46.4910	3.67	0.2417	0.3631
			341296	3.079	92.3820	7.3	0.4803	0.3642
		NdFeB	170648	1.539	18.3120	6.82	0.0365	0.0239
	Iron		341296	1.539	38.4925	14.33	0.7672	0.0239
	(99.8)	Sm_2Co_{17}	170648	1.539	18.3120	6.82	0.0365	0.0239
4			341296	1.539	38.4925	14.33	0.7672	0.0239
		NdFeB	170648	3.849	61.5880	6.17	0.4562	0.3306
	Iron		341296	3.849	107.779	10.79	0.7983	0.3306
	(99.95)	Sm_2Co_{17}	170648	3.849	61.5880	9.17	0.3069	0.1496
			341296	3.849	107.779	16.05	0.5370	0.1496
		NdFeB	170648	0.811	3.24600	2.45	0.0035	0.0080
	Iron		341296	0.811	8,12250	6.11	0.0088	0.0080
	(99.8)	Sm_2Co_{17}	170648	0.811	3.24600	2.45	0.0035	0.0080
5			341296	0.811	8,12250	6.11	0.0088	0.0080
		NdFeB	170648	0.970	8.11500	5.12	0.0106	0.0114
	Iron		341296	0.970	14.6070	9.21	0.0191	0.0114
	(99.95)	Sm_2Co_{17}	170648	0.970	8.1150	5.12	0.0106	0.0114
			341296	0.970	14.607	9.21	0.0191	0.0114
		NdFeB	170648	0.811	4.6890	4.04	0.0053	0.0073
	Iron		341296	0.811	9.7380	8.07	0.0106	0.0073
	(99.8)	Sm_2Co_{17}	170648	0.811	4.6890	4.04	0.0053	0.0073
6			341296	0.811	9.7380	8.07	0.0106	0.0073
		NdFeB	170648	0.970	9.7380	6.75	0.0127	0.0104
	Iron		341296	0.970	16.230	11.25	0.0212	0.0104
	(99.95)	Sm_2Co_{17}	170648	0.970	9.7380	6.75	0.0127	0.0104
			341296	0.970	16.230	11.25	0.0212	0.0104
		NdFeB	170648	0.649	2.4340	0.38	0.0018	0.0278
	Iron		341296	0.649	6.4920	1.01	0.0049	0.0278
	(99.8)	Sm_2Co_{17}	170648	0.649	2.4340	0.38	0.0018	0.0278
7			341296	0.649	6.4920	1.01	0.0049	0.0278
	Iron	NdFeB	170648	0.811	6.4920	0.71	0.0071	0.0568
	(99.95)		341296	0.811	12.984	1.41	0.0142	0.0368
	Iron	NdFeB	170648	0.568	3.2460	0.71	0.0071	0.0568
8	(99.95)		341296	0.568	8.1150	1.41	0.0142	0.0368
		Sm_2Co_{17}	170648	0.568	3.2460	0.88	0.0035	0.0080

4 CONCLUSION

Fem analysis is done for magnetic circuit analysis of PMH stepper motor using PDE toolbox of Matlab whose responces are shown in Fig.2, Fig.3, Fig.4 and Fig.5 for first two topologies.Equinalent circuit model analysis is used for gap permeance, steady state, cogging torques and instantaneous torque analysis whose responces are shown in Fig.7, Fig.8, Fig.9 and Fig.10, Fig.11, Fig.12 respectively. Similarly investigation carried for 8 topologies. Finally for getting rated steady state torque (1.5 Nm) with low THD , low uniform air-gap (0.137 mm) with extra stator teeth on stator (topology 1) with iron (99.95%) for stator and rotor cores with current density of 341296 A/m^2 (1 A for 36 SWG) is investigated. Cogging torque to Steady state torque ratio (4.77%) is not effected by variation of permanent magnet material for the above topology. Cogging torque can be minimized by providing extra teeth on stator.

REFERENCES

[1] K. R. Rajagopal, M. Krishnaswammy, Bhim Singh and B. P. Singh, '*An Improved High- Resolution Hybrid Stepper Motor for Solar-Array Drive of Indian Remote- Sensing Satellite*', IEEE transactions on Industry Applications, Vol. 33, No. 4, July/August 1997

[2] Praveen R.P, Ravichandran M.H, V. T. Sadasivan Achari, Dr.Jagathy Raj V. P, Dr.G.Madhu and Dr.G.R. Bindu6, '*Design and Finite Element Analysis of Hybrid Stepper Motor for Spacecraft Applications*', 978-1-4244-4252-2/09, IEEE, 2009

[3] Dou Yiping, '*The Engineering Rationality of a Hybrid Stepping Motor Calculation Model*', Proceedings of theCSEE, vol. 19, no. 5, pp. 35-38, May 1999.

[4] Fengge Zhang, Ningze Tong, Fengxiang Wang, '*Study on Cogging Torque Reduction Methods of PM Stepping Motor*', IEEE International Conference on Power System Technology, POWERCON 2004, Singapore, 21-24 November 2004
[5] K. C. Mukharji, '*Magnetic Permeance of Identical Double Slotting Deduction from Analysis by F. W. Carter*', IEE, volume 118, No.9, September 1971.
[6] H. D. Chai, '*A Mathematical Model **for** Single-Stack Step Motors*', IEEE Transactions on Power Apparatus and Systems, Vol. PAS-94**,** no. 5, September/October 1975.
[7] Nobuyuki Matsui, '*Instantaneous Torque Analysis of Hybrid Stepping Motor*', IEEE transactions on Industry Applications, Vol. 32, No. 5, September/October 1996

Bibliography of Authors

Mr.E.V.C.Sekhar Rao graduated in Electrical & Electronics Engg from Jawaharlal Nehru Technological University, Hyderabad in the year 1999, post-graduated from Osmania University, Hyderabad in industrial drives and control in 2005 and pursuing his PHD in Osmania university. He has 12 years of industrial experience and ten years of academic experience. His areas of interest are Electrical machine design and Special machines. At present he is assistant professor in the department of Electrical & Electronics Engineering in CBIT, Hyderabad; India.He presented technical papers in IIT, Delhi and MGR university, Chennai in IEEE and IET international conferences respectively.

Dr.P.V.N.Prasad graduated in Electrical & Electronics Engineering from Jawaharlal Nehru Technological University, Hyderabad in 1983 and received M.E in Industrial Drives & Control from Osmania University, Hyderabad in 1986. He served as faculty member in Kothagudem School of Mines during 1987 - 95 and at presently serving as Professor in the Department of Electrical Engineering, Osmania University, Hyderabad;India. He received his Ph.D in Electrical Engineering in 2002. His areas of interest are Reliability Engineering and Computer Simulation of Electrical Machines & Power Electronic Drives. He is recipient of Dr.Rajendra Prasad Memorial Prize, Institution of Engineers (India), 1993 - 94 for best paper. He has got over 65 publications in National Journals & Magazines and International Conferences & Symposia and presented technical papers in Thailand, Italy, USA, and Singapore.